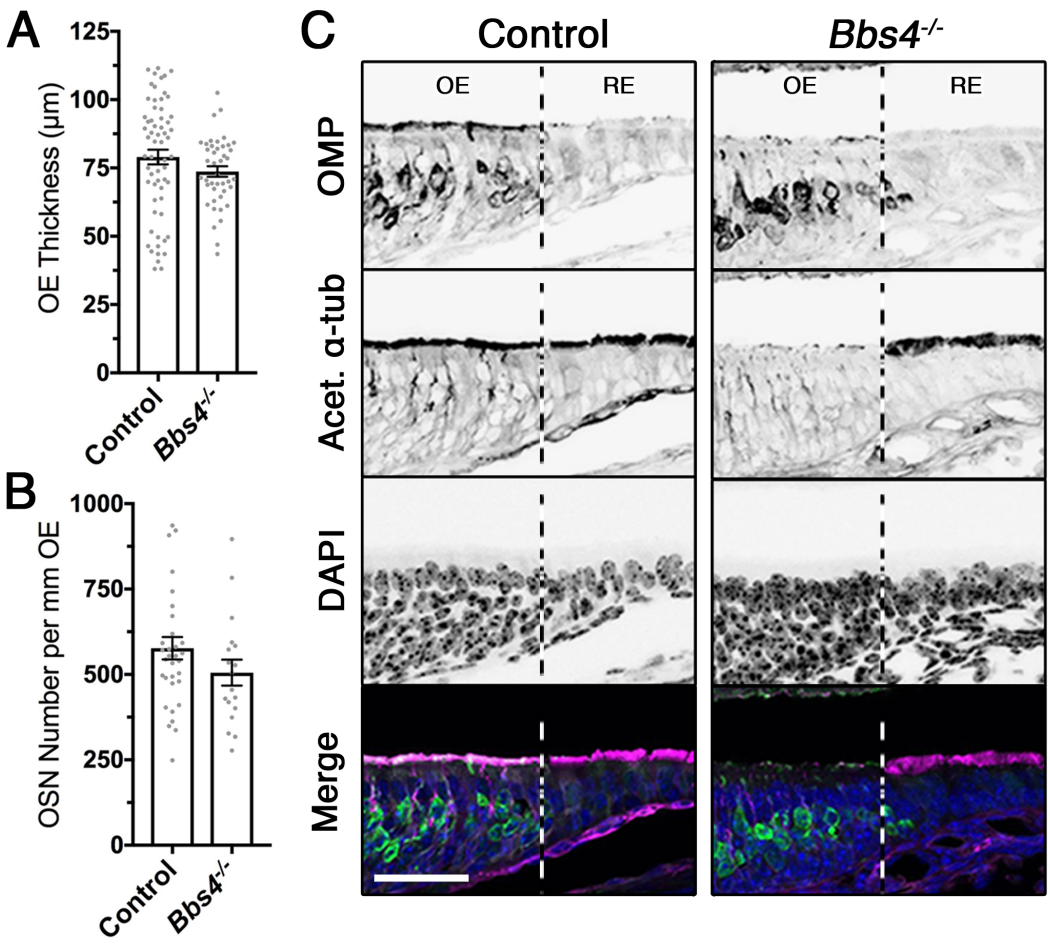

Figure S1. OE thickness and OSN density are unchanged in *Bbs4*$^{-/-}$ mutant mice.

(A) Quantification of OE thicknesses was unchanged between P20-35 control and *Bbs4*$^{-/-}$ mutant OE (n = 7 WT, 5 KO; t(104)=1.472, P=0.1440, Unpaired t-test). (B) Quantification of OSN counts per mm of OE was unchanged between P20-35 control and *Bbs4*$^{-/-}$ mutant OE (n = 7 WT, 5 KO; t(49)=1.357, P=0.1811, Unpaired t-test). (C) Representative sections of the olfactory and respiratory epithelia border from (left) control and (right) *Bbs4*$^{-/-}$ mutant mice, immunostained for (top) OMP, (middle-top) acetylated α-tubulin, (middle-bottom) DAPI, and (bottom) merged. Dashed lines demarcate the OE and RE boundary. Scale bar = 40 µm.

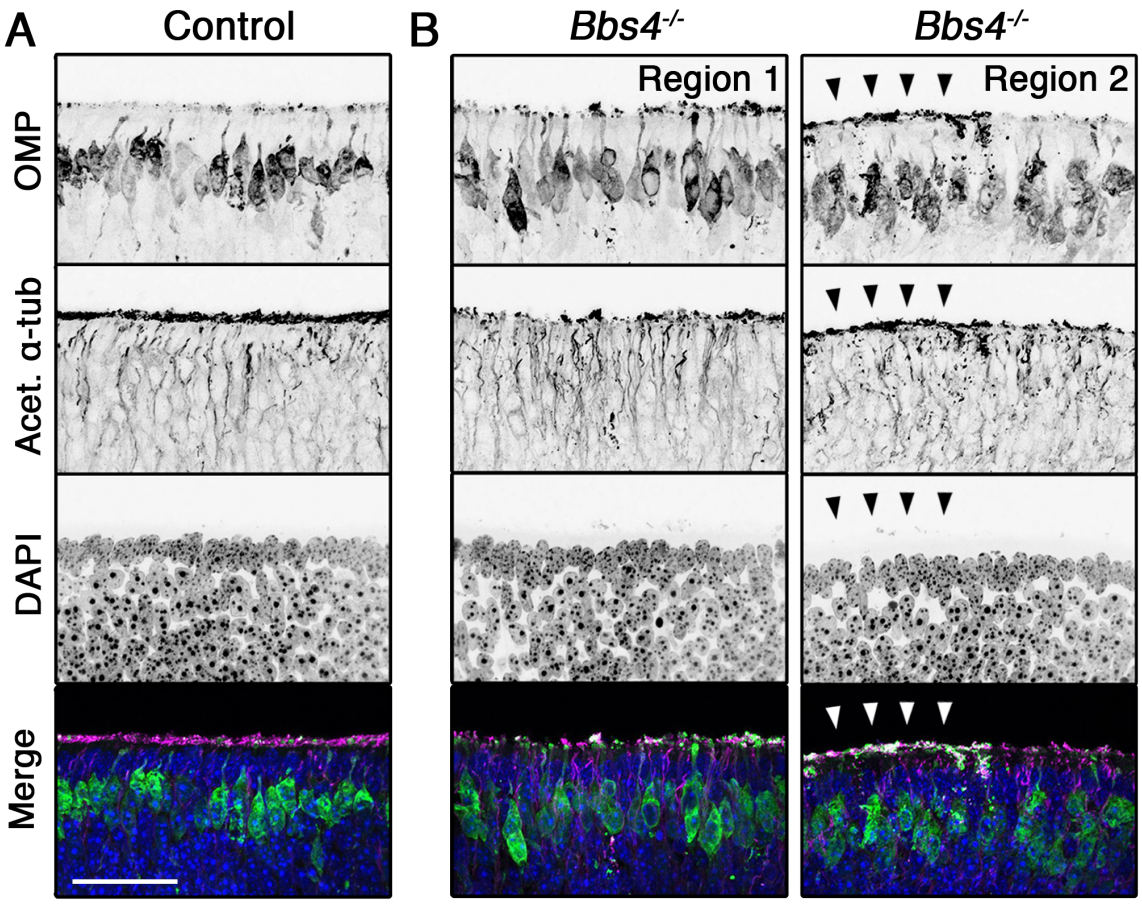

Figure S2. Ciliary degeneration within early postnatal *Bbs4*$^{-/-}$ mutant OE.

(A) Representative OE from postnatal 5-day-old (P5) (left) control and (middle, right) *Bbs4*$^{-/-}$ mutant mice immunostained for (top) OMP, (middle-top) acetylated α-tubulin, (middle-bottom) DAPI, and (bottom) merged. Although *Bbs4*$^{-/-}$ mutant mice largely lack apical acetylated α-tubulin immunostaining, some regions retain residual cilia (arrowheads). Scale bar = 40 µm.

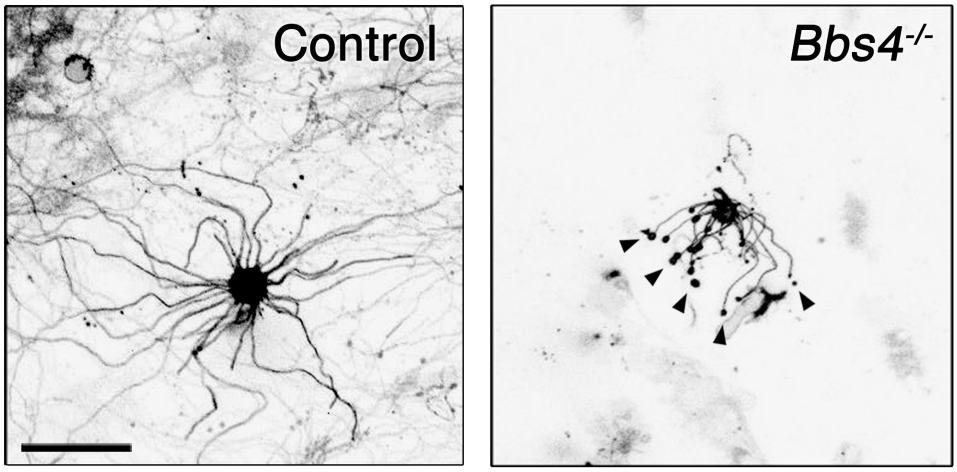

Figure S3. *Bbs4*$^{-/-}$ mutant OSNs display enlargement of distal ciliary tips.

Representative live *en face* confocal images of ectopically expressing myristoylated-palmitoylated-mCherry (MP-mCh) in OSN cilia from (left) control and (right) *Bbs4*$^{-/-}$ mutant mice. In rare instances, *Bbs4*$^{-/-}$ mutant OSNs exhibit engorged swellings at the ciliary tip (arrowheads), larger than those observed in some wild type control OSNs. Scale bar = 20 µm.

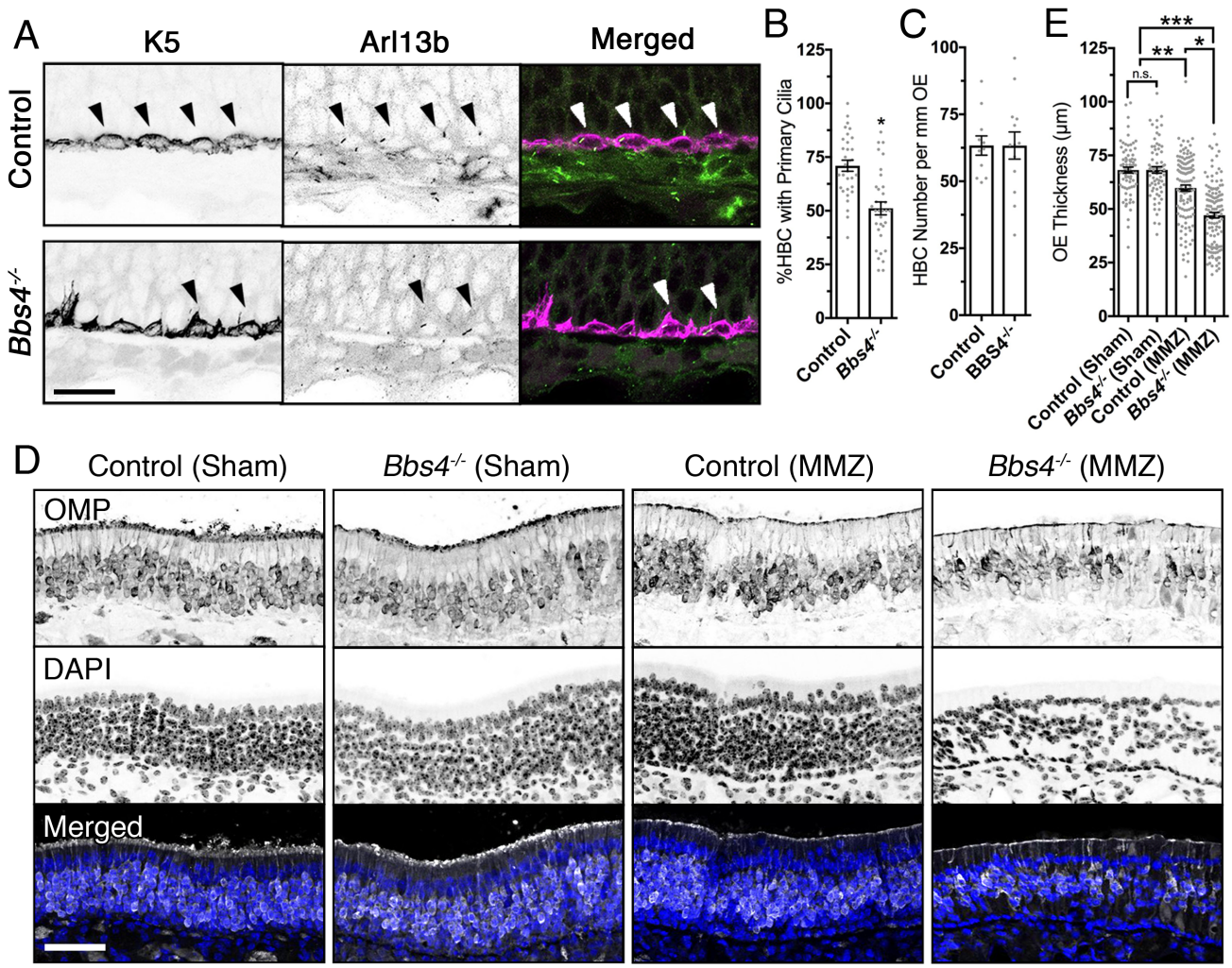

Figure S4. *Bbs4*$^{-/-}$ mutant mice have reduced regenerative capacity after ablation.

(A) Representative images of ciliated horizontal basal cells (HBCs; arrowheads) at the base of the OE from control (top) and *Bbs4*$^{-/-}$ mice (bottom). Tissue was immunostained for (left) cytokeratin-5 (K5) to label HBCs, (middle) Arl13b to label primary cilia, and (right) merged. (B) Quantification of ciliated HBCs demonstrated a 30% decrease in *Bbs4*$^{-/-}$ mice (71.0 ± 2.6 ciliated/total HBCs) compared to control (51.2 ± 3.0 ciliated/total HBCs; n = 4 WT, 5 KO; t(64)=5.0, *, P<0.0001, Unpaired t-test). (C) Quantification of HBC number per millimeter of OE exhibited no difference between control (63.4 ± 3.6 cells/mm) and *Bbs4*$^{-/-}$ mice (63.3 ± 5.1 cells/mm; n = 4 WT, 5 KO; t(22)=0.003, P=0.998, Unpaired t-test). (D) Representative cross sections of the OE immunostained for OMP from sham-treated control and *Bbs4*$^{-/-}$ mutant mice, and methimazole-treated control and *Bbs4*$^{-/-}$ mutant mice. (E) Quantification of OE thicknesses from sham treated control (68.14 ± 1.39 µm; n = 4) and *Bbs4*$^{-/-}$ mutant (68.20 ± 1.54 µm; n = 5), methimazole (MMZ)-treated control (59.75 ± 1.44 µm; n = 4) and *Bbs4*$^{-/-}$ mutant (47.1 ± 1.32 µm; n = 4) (F(3,382)=49.91, P<0.0001, One-way ANOVA, Tukey Post-hoc, n.s., P>0.05, *, P<0.0001, **, P<0.0005, ***, P<0.0001). Scale bar = 5 µm (A), 50 µm (D).

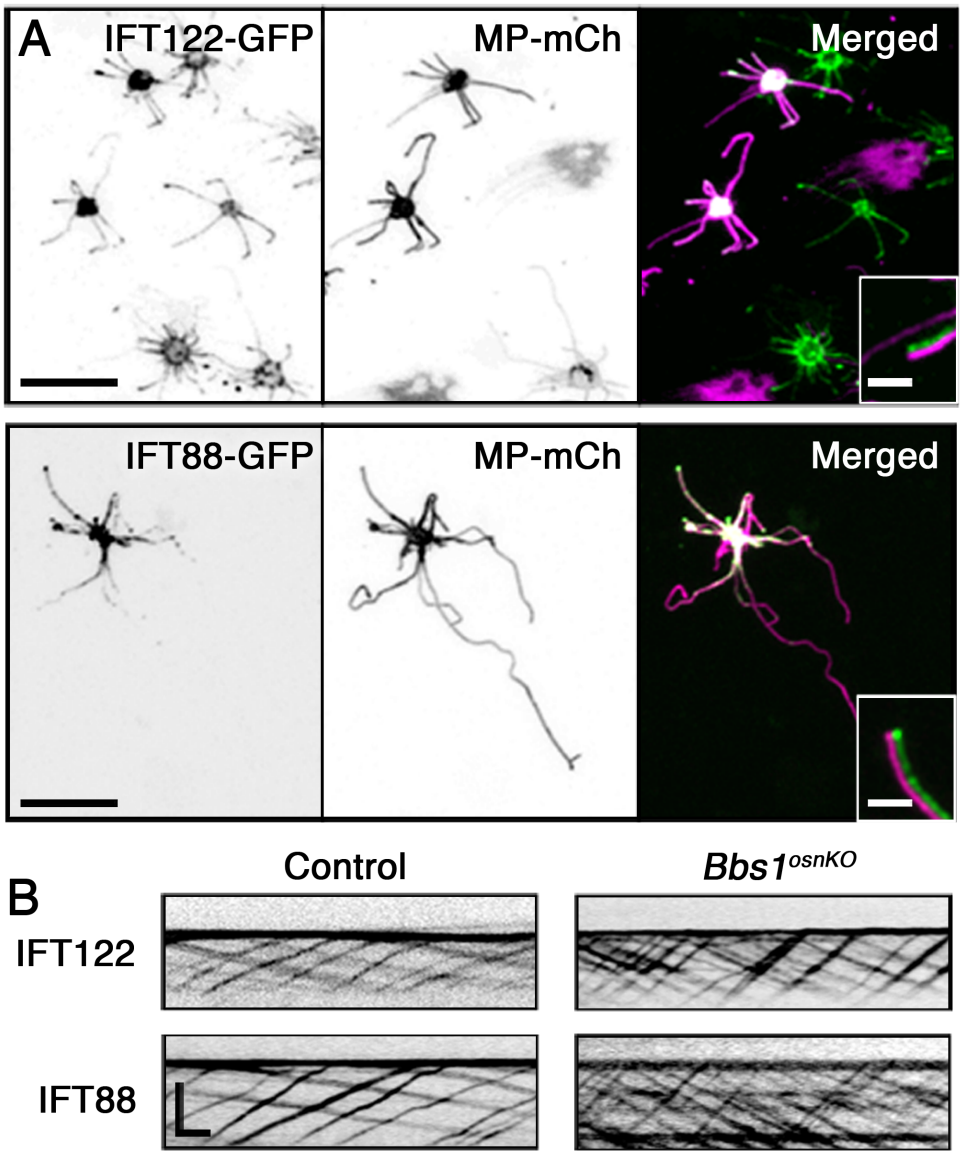

Figure S5. Decoupling of IFT trafficking in *Bbs1KO* mice.

(A) Representative confocal *en face* images of OSNs from *Bbs1KO* mice. Imaged OSNs were ectopically expressed (top) IFT122-GFP and (bottom) IFT88-GFP with MP-mCh a full-length cilia marker. (B) Representative kymograms from control and *Bbs1KO* mice ectopically expressing (top) IFT122-GFP and (bottom) IFT88-GFP. Compared to control recordings, *Bbs1KO* mice demonstrated increased IFT122 and IFT88 trafficking velocities. Scale bar = 10 µm, 2.5 µm, 10 s x 5 µm (kymogram-B).